Histochem Cell Biol (2017) 148:299–311
DOI 10.1007/s00418-017-1585-1

ORIGINAL PAPER

Laser capture microdissection protocol for gene expression analysis in the brain

P. Garrido-Gil[1,2] · P. Fernandez-Rodríguez[1] · J. Rodríguez-Pallares[1,2] · Jose L. Labandeira-Garcia[1,2]

Accepted: 24 May 2017 / Published online: 31 May 2017
© Springer-Verlag Berlin Heidelberg 2017

Abstract Laser capture microdissection (LCM) allows the isolation of specific cell populations from complex tissues that can be then used for gene expression studies. However, there are no reproducible protocols to study RNA in the brain and, particularly, in the substantia nigra. RNA is a very labile biomolecule that is easily degraded during manipulation. LCM studies use low amounts of material and special precautions must be taken to preserve RNA yield and integrity, which are decisive for PCR analysis. The RNA yield and/or integrity can be affected negatively by tissue manipulation, LCM process and RNA extraction. We have optimized these three critical steps using nigral tissue sections, and developed a LCM protocol to obtain high-quality RNA for gene expression analysis. The optimal LCM protocol requires the use of 20 µm-thick tissue sections mounted on glass slides and processed for rapid tyrosine hydroxylase immunofluorescence. Additionally, a total microdissected tissue area of 1 mm^2 and a column-based RNA extraction method were used to obtain a high RNA yield and integrity. In the rat substantia nigra, we demonstrated the expression of RNA for the angiotensin type 1 and type 2 receptors using this optimized LCM protocol. In conclusion, the LCM protocol reported here can be used to study the expression of both scarcely or abundantly expressed genes in the different brain regions of mammals under both physiological and pathological conditions.

✉ Jose L. Labandeira-Garcia
joseluis.labandeira@usc.es

[1] Laboratory of Neuroanatomy and Experimental Neurology, Department of Morphological Sciences, CIMUS, University of Santiago de Compostela, 15782 Santiago De Compostela, Spain

[2] Research Center on Neurodegenerative Diseases (CIBERNED), Madrid, Spain

Keywords Laser capture microdissection · RT-PCR · Brain · Substantia nigra · Gene expression · RNA integrity and yield

Introduction

The laser capture microdissection (LCM) technique was developed due to carry out molecular studies from specific cell populations located in complex tissue sections. The first LCM system consisted of an inverted microscope and an infrared laser. Additionally, a camera connected to a computer allowed for visualizing the process (Emmert-Buck et al. 1996). This method was initially commercialized by Arcturus as the PixCell system (Decarlo et al. 2011; Sluka et al. 2008). Afterwards, the LCM methodology was optimized and different LCM systems were commercialized. The PALM Microbeam system (Zeiss), together with Arcturus system, is the most commonly used LCM systems. The major advantage of the PALM system is that there is no direct contact between the collection microtube and the sample. This system uses an ultraviolet laser that reaches the sample through the microscope objective and cuts and catapults the tissue to the microtube cap (Decarlo et al. 2011; Sluka et al. 2008).

Both LCM systems have been used for gene expression studies in different tissues, including the brain (Cheng et al. 2013; Elkahloun et al. 2016; Espina et al. 2006; Kerman et al. 2006; Kim et al. 2015). Although, combination of LCM with DNA analysis has been widely used (Curran et al. 2000; Fend and Raffeld 2000; Korabecna et al. 2016; Li et al. 2017), its combination with RNA studies has technical problems, which lead to a restricted use (Esposito 2007; Field et al. 2011). In addition, LCM protocols recommended by major LCM system manufacturers are

hardly reproducible, and each new user has to develop new experimental methodologies adapted for the specific LCM system and the type of tissue studied.

The yield (concentration per tissue quantity) and integrity of the RNA obtained after the microdissection process are decisive for the subsequent use of this biomolecule in gene expression studies (Kerman et al. 2006). Since LCM and gene expression studies use low amounts of material, special cautions are necessary to preserve RNA yield and integrity, which can be negatively affected by sample manipulation before (i.e., cutting, staining), during (i.e., microdissection protocol and capture success) and after (i.e., RNA extraction method) the LCM process (Decarlo et al. 2011). However, there is a lack of comparative studies to clarify the most appropriate methods for staining, LCM (section thickness, slide type, microdissected tissue quantity, capture success), and RNA extraction to obtain enough amount of high-quality RNA for gene expression studies. In the present study, we will use substantia nigra (SN) tissue sections to optimize these critical steps.

The SN is a dopaminergic nucleus located in the ventral midbrain and involved in motor control and other brain functions. Degeneration of the nigral dopaminergic neurons leads to motor deficits in Parkinson's disease (PD). Previous human postmortem and animal studies demonstrated the existence of cellular subpopulations within the SN showing a differential vulnerability to neurodegeneration (Damier et al. 1999; Gonzalez-Hernandez et al. 2004, 2010; Haber 2014). Dysregulation of the brain renin–angiotensin system activity and changes in the expression of the angiotensin type 1 (AT1) and type 2 (AT2) receptors have been associated with pathogenesis of PD and could explain the differential vulnerability of dopaminergic subpopulations (Labandeira-Garcia et al. 2011, 2012, 2014). Therefore, LCM followed by PCR analysis could be an interesting approach to investigate this complex midbrain nucleus. Consistent with this, we used our optimized LCM method to analyze the expression of angiotensin AT1 and AT2 receptor mRNA, which are normally expressed at low levels in the healthy SN.

Materials and methods

Animals and ethical aspects

Twelve adult (10-week old) male Sprague–Dawley rats were included in the present study. The animals were housed in conditions of constant room temperature (21–22 °C) and a 12 h light/12 h dark cycle and given free access to food and water. All experiments were performed according to the European and Spanish Directives (2010/63/EU and RD/53/2013, respectively) for the protection of animals used for scientific purposes. The experimental design was approved by the corresponding Ethical Committee at the University of Santiago de Compostela.

Experimental design

In the first series of experiments, we evaluated (before the microdissection process) the effect of the tyrosine hydroxylase (TH) immunostaining protocol (immunofluorescence or immunohistochemistry) and/or the duration of immunostaining incubations on the yield and integrity of the RNA obtained from scraped SN tissue sections ($n = 4$–5 per group).

In the second series of experiments, we examined the effect, before the microdissection process, of neutral red staining and the TH immunostaining on the yield and integrity of the RNA obtained from scraped SN tissue sections ($n = 4$–5 per group).

In the third series of studies, we investigated the effect of tissue section thickness (10 or 20 µm) and/or slide type (glass or PEN membrane-coated) on the capture success of microdissected tissue and the RNA yield and integrity obtained after the LCM process ($n = 4$–5 per group).

In the fourth series of experiments, we investigated the effect of the microdissected tissue area (0.4 or 1 mm^2) and/or the RNA extraction method (phase separation or column-based) on the RNA yield and integrity obtained after LCM ($n = 4$–5 per group). Finally, in the fifth series of experiments, we used the optimized staining, LCM, and RNA extraction conditions to determine the expression of AT1 and AT2 receptors and the dopaminergic markers TH, dopamine transporter (DAT), and dopamine receptor type 2 (D2R) in the rat SN ($n = 6$).

Tissue preparation for laser microdissection

Animals were sacrificed by decapitation. Their brains were rapidly removed, immediately embedded in OCT, frozen in liquid nitrogen and stored at −80 °C until further processing. Then, serial coronal sections (10 or 20 µm thick) containing the substantia nigra were cut at −20 °C using a cryostat (Thermo Scientific). The sections were mounted on glass slides (Marienfeld) or on slides covered with a polyethylene naftelato (PEN) membrane (PEN1.0, Zeiss). Slides were allowed for complete dehydration in the cryostat chamber for 10 min. Then, slides were stored (for no longer than 1 week) at −80 °C inside sterile plastic containers with silica gel to prevent tissue hydration until further processing. Previously, the glass and membrane slides had been treated to remove any RNAse contamination. Briefly, glass slides were successively exposed to ultraviolet (UV) light (10–15 min) and high temperatures (2 h at 220 °C). In contrast, membrane-covered slides were treated

with RNase AWAY (Thermo Fisher) for 5 min. After being washed with diethylpyrocarbonate (DEPC; Sigma) water (2 × 10 min), the slides were incubated for 2 h at 37 °C and, finally, they were exposed to UV light for 15 min.

Neutral red staining

Slides containing nigral tissue sections were stained with a rapid protocol for neutral red. Briefly, tissue sections were fixed in 70% ethanol for 30 s, hydrated in DEPC water and then stained with a 1% neutral red solution in DEPC water for 2 min. Sections were then dehydrated by quick dips in graded ethanol (50-70-96-100% in DEPC water). Then, tissue sections were immersed in xylene for 4 min to achieve complete dehydration. Finally, sections were dried at room temperature for 3 min and immediately processed with the microdissection system. All steps were performed on ice. For each experimental day, all aqueous regents were freshly prepared with DEPC water (RNase free).

Immunofluorescence labeling for tyrosine hydroxylase (TH)

Slides containing nigral tissue sections were stained with three different protocols for TH immunofluorescence labeling based on the duration of incubations: (i) an ordinary over night (o.n.) primary antibody incubation (i.e., 2-day total protocol duration) (ii) a shorter 1 h incubation (1-day total protocol duration), and (iii) a rapid 5-min incubation (20 min total duration protocol). Briefly, SN tissue sections were fixed in acetone for 40 s, hydrated in phosphate buffer saline (PBS) and, then, incubated with a mouse monoclonal antibody against the dopaminergic marker TH (Sigma) diluted 1:5000 (i and ii) or 1:100 (iii). After being washed with PBS, tissue sections were incubated 2 h (i), 1 h (ii) or 5 min (iii) with a goat anti-mouse Cy3-conjugated secondary antibody (Chemicon) diluted 1:200 (i and ii) or 1:25 (iii). Incubation of tissue sections with primary and secondary antibodies was performed in a moist chamber. SN containing sections were, then, dehydrated by quick dips in graded ethanol (50-70-96-100%). Then, tissue sections were immersed in xylene for 4 min to achieve complete dehydration. Finally, sections were allowed to dry at room temperature for 3 min and immediately processed with the microdissection system. All steps (except xylene immersion) were performed on ice and all aqueous regents were freshly prepared with DEPC water (RNase free) for each experimental day.

Immunohistochemistry for tyrosine hydroxylase

Nigral tissue sections were stained with three different protocols for TH immunohistochemistry based on the duration of incubations: (i) an ordinary o.n. incubation, (ii) a 1 h incubation and (iii) a rapid protocol (i.e., 5 min incubation). Slides containing SN tissue sections were fixed in acetone for 40 s and, then, hydrated in PBS. Subsequently, tissue sections were incubated in a solution of hydrogen peroxide (H_2O_2, 3%; Merck) for inhibition of endogen peroxidase activity and, then, incubated o.n. for (i), 1 h (ii) or 5 min (iii) with a mouse monoclonal antibody against TH diluted 1:10000 (i and ii) or 1:200 (iii). After being washed with PBS, tissue sections were incubated for 1 h (i and ii), or 5 min (iii) with a biotinylated horse anti-mouse secondary antibody (Vector laboratories) diluted 1:200 (i and ii) or 1:25 (iii). Tissue sections were then incubated with the avidin–biotin peroxidase complex (1:70; Vector Laboratories) for 1 h (i and ii) or 5 min (iii). Staining for peroxidase was performed in PBS with 0.05% diaminobenzidine tetrahydrochloride (Sigma) and 0.04% H_2O_2. All incubations of tissue sections were performed in a moist chamber. SN-containing sections were, then, dehydrated by quick dips in graded ethanol (50-70-96-100%). Then, tissue sections were immersed in xylene for 4 min to achieve complete dehydration. Finally, sections were allowed to dry at room temperature for 3 min and immediately processed with the microdissection system. All steps (except peroxidise staining and xylene immersion) were performed on ice and all aqueous regents were freshly prepared with DEPC water (RNase free) for each experimental day.

Laser capture microdissection

Laser capture microdissection (LCM) was performed using a PALM MicroBeam system (Zeiss) consisting of an inverted microscope with a motorized stage, an ultraviolet (UV) laser and an X-Cite 120 fluorescence illuminator (EXFO). The microdissection process was visualized with an AxioCam Icc camera coupled to a computer and controlled by a Palm RoboSoftware. Specifically, the SN was visualized under bright-field (neutral red staining) or fluorescence (TH immunofluorescence) microscopy with a 20× objective. An area of 0.4 or 1 mm^2 was selected using the PALM RoboSoftware, and cut and catapulted by laser pulses into an adhesive microtube cap (Zeiss). The capture success of microdissected tissue was defined as the ability of the laser to dissect the cells of interest and catapult them to the microtube cap. The capture success was expressed as a percentage and was calculated by dividing the tissue area dissected by the tissue area previously marked with the software tool. Three classes of capture success were established: good (+++), when a 100% of the selected tissue was microdissected; fair (++), when less than 100% of the marked tissue was microdissected; and bad (+), when less than 50% of the selected tissue was microdissected. The capture success was evaluated for each tissue section and

LCM protocol by checking the slide before and after the microdissection process. Furthermore, observation of the microtube cap after LCM was used to confirm the capture success.

RNA extraction

Total RNA extraction was performed using two different methods: a method based on phase separation (Trizol reagent, Life Technologies) and a method based on separation by spin columns (RNeasy Micro kit, Qiagen).

RNA extraction based on phase separation (Trizol method)

After being collected into the microtube cap, the microdissected tissue was immediately disrupted and homogenized by incubating microtubes upside down with 500 µl of Trizol reagent under agitation at room temperature (RT) for 30 min. Homogenized tissue was spun down by centrifugation (12000 rpm, 5 min, 4 °C) and stored at −80 °C until resuming all samples RNA extraction. Then, 100 µl of chloroform (Sigma) was added to the Trizol containing lysates and the mixes were incubated for 2 min. Subsequently, microtubes were centrifugated at 12,000*g* and 4 °C for 15 min and the aqueous phase containing RNA was separated. Then, the RNA was precipitated by the addition of glycogen (0.6 µl, Roche) and isopropanol (250 µl, Sigma) to the aqueous phase, the incubation of the microtubes for 10 min at room temperature and their centrifugation at 12,000*g* and 4 °C for 10 min. The precipitated RNA was, first, washed twice with 75% ethanol and, then, solubilized in 14 µl of DEPC water.

RNA extraction based on spin columns (RNeasy Micro kit)

Microdissected tissue was disrupted and homogenized by incubating microtubes upside down with 350 µl of the lysis buffer RLT (Qiagen) containing β-mercaptoethanol for 30 min under agitation at room temperature (RT). Homogenized cells were spun down by centrifugation (12,000 rpm, 5 min, 22 °C) and stored at −80 °C until resuming all samples RNA extraction. Then, 350 µl 70% ethanol was added to the lysate, the mix was centrifugated into an RNeasy MinElute spin column (15 s at 8000*g*) and the flow-through was discarded. Columns were then treated with DNAse I to remove genomic DNA and they were washed twice. Finally, RNA was eluted in 14 µl of RNAse-free water.

Measurement of RNA yield and integrity

The yield and integrity of total isolated RNA from microdissected samples were measured using a 2100 Bioanalyzer (Agilent Technologies). Total RNA (1 µl per sample) was, first, denatured (70 °C, 2 min) and, then, loaded into a RNA 600 Nano or Pico chip (Agilent Technologies) according to the manufacturer's instructions. The RNA concentration of each sample was obtained with the 2100 Bioanalyzer. Then, concentration was divided by the tissue area value to calculate the RNA yield. Additionally, the RNA Integrity Number (RIN) was calculated by the 2100 Bioanalyzer according to an algorithm from Agilent Technologies (Kerman et al. 2006; Schroeder et al. 2006). A RIN value was obtained for each sample on a scale of 1–10 as an indication of RNA quality. The RNA quality is considered excellent for RIN $\geq$ 7, good for RIN $\geq$ 5 and poor for RIN < 5 (Kerman et al. 2006; Schroeder et al. 2006). In addition, the RIN shows a strong correlation to the RT-PCR experiments and allows for a straightforward separation into acceptable and unacceptable RT-PCR results. The meaningful threshold value for the RIN that separates positive from negative RT-PCR results is 5 (Schroeder et al. 2006).

Reverse transcription

All the RNA obtained for each sample was used for the reverse transcription. Initially RNA was denaturalized at 65 °C for 10 min. Then, a reaction mix was added to RNA to a final reaction volume of 30 µl, and the samples were incubated for 1 h at 37 °C. The reaction was stopped in ice and the cDNA stored at −80 °C. Reaction mix contained the M-MLV reverse transcriptase (1.67 U/µl; Invitrogen) and its first-strand buffer (50 mM Tris–HCl pH 8.3, 75 mM KCl, 3 mM MgCl), a mixture of hexanucleotides as random primers (5 µg/ml, Invitrogen), a deoxynucleotide triphosphate mix (dNTPs; 0.3 mM; Invitrogen), the M-MLV stabilizer DTT (6.6 mM; Invitrogen) and the RNAse OUT enzyme (1.33 U/µl; Invitrogen).

Real time polymerase chain reaction (RT-PCR)

SYBR Green Master Mix (Bio-Rad) containing iTaq DNA polymerase, deoxynucleotides and $MgCl_2$ was used for RT-PCR. cDNA and the specific primer pairs (0.165 µM; Sigma) were added to the SYBR Green Master Mix at a final volume of 50 µl. PCR was performed using an iCycler real time PCR platform (Bio-Rad). Initially, cDNA was denatured during 3 min at 95 °C. Then, DNA was amplified during 40 cycles including an annealing/extension step (60 °C, 30 s) and a denaturation step (95 °C, 10 s). Finally, the temperature declined (0.5 °C per min) until reaching 65 °C. The PCR products were loaded into a 2% agarose gel with Syber Safe (Invitrogen), separated by electrophoresis and visualized with an UV detection system (Molecular Imager Chemidoc XRS System, BioRad). Primer sequences were as follows: for AT1, forward 5′-TTCAACCTCTACGCCAGTGTG-3′,

reverse 5′-GCCAAGCCAGCCATCAGC-3′; for AT2, forward 5′-AACATCTGCTGAAGACCAATAG-3′, reverse 5′-AGAAGGTCAGAACATGGAAGG-3′; for TH, forward 5′-GGCTTCTCTGACCAGGTGTATCG-3′, reverse 5′-GCAATCTCTTCCGCTGTGTATTCC-3′; for DAT, forward 5′-CGACTCTGTGAGGCATCTGTG-3′, reverse 5′-GGAAGGAGAAGACGACGAAGC-3′; for D2R, forward 5′-AGACGATGAGCCGCAGAAAG-3′, reverse 5′-GCAGCCAGCAGATGATGAAC-3′;for GAPDH, forward 5′-GCAAGTTCAACGGCACAGTCAAG-3′, reverse 5′-ACATACTCAGCACCAGCATCACC-3′.

Statistical analysis

All data were obtained from at least three independent experiments and were expressed as mean values ± SEM. Comparisons of three or more groups were carried out by one-way ANOVA (for single variable analysis) followed by the Student–Newman–Keuls post hoc test or two-way ANOVA (for multiple variables analysis) followed by the Bonferroni post hoc test. The normality of populations and homogeneity of variances were tested before each ANOVA. Differences were considered statistically significant at $p \leq 0.05$. Statistical analyses were carried out with SigmaStat 3.0 (Jandel Scientific, San Rafael, CA, USA).

Results

Effect of the TH immunostaining protocol and duration of antibody incubation on the RNA yield and integrity before LCM

Five tissue sections per animal containing the SN were processed for different TH immunofluorescence or immunohistochemistry protocols based on the duration of immunostaining incubations. Then, SN sections were scraped from the slides with the aid of a scalpel to determine the effect of these different immunostaining protocols on the RNA yield (concentration per section) and integrity (RIN) before LCM. Tissue sections without staining were used as controls. RNA from control tissue sections showed a yield of 36.8 ± 6.7 ng/µl per section and a RIN of 7.8 ± 0.1, indicative of an excellent RNA quality (Fig. 1a, b). Tissue sections processed for rapid (using a 5 min primary antibody incubation) immunofluorescence or immunohistochemistry (immunoperoxidase) staining method showed similar RNA yield (37.6 ± 1.7 or 37.8 ± 13 ng/µl per section, respectively) compared with control sections (Fig. 1a). Note, however, that the RNA yield obtained from sections processed for the rapid immunohistochemical method showed great variation, which was reflected by the high

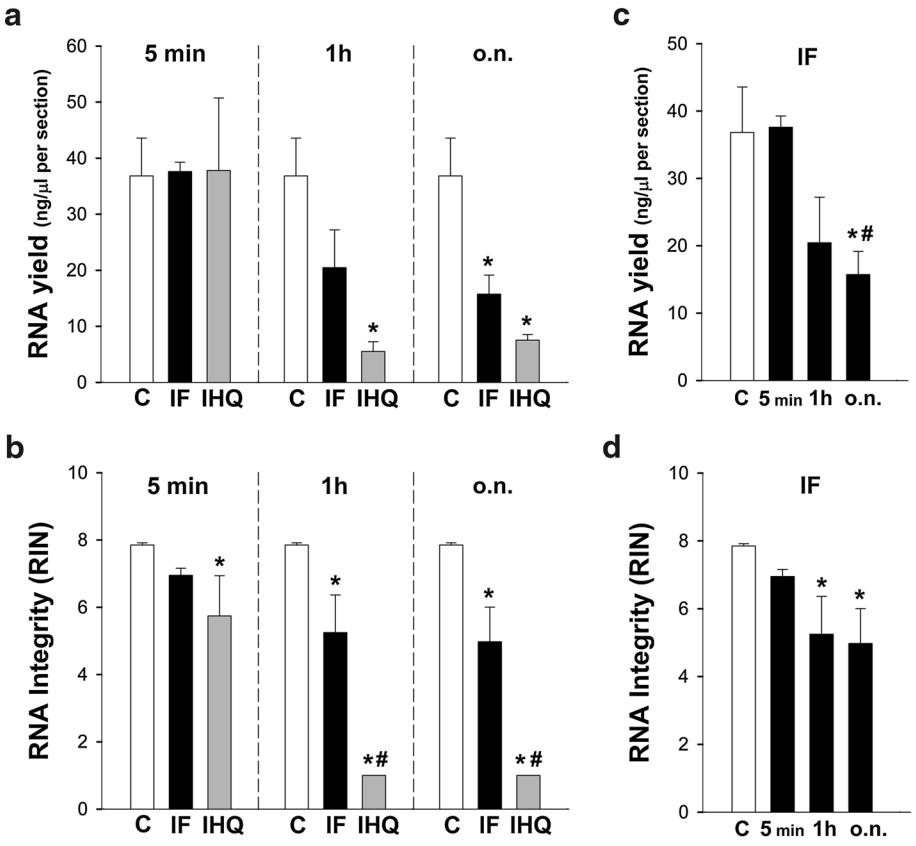

Fig. 1 The RNA obtained from SN sections processed for rapid TH immunofluorescence (IF) or immunohistochemistry (IHQ) showed similar yield compared with control sections (**a**). However, longer IF or IHQ protocols decreased RNA yield compared with the control group (**a**). With regard to the RNA integrity (**b**), only rapid TH IF, but not rapid IHQ or longer protocols, allowed for preserving the RIN value at control levels. The comparison of different duration IF protocols is highlighted in **c** and **d**, and shows that the shortened IF protocol led to the best RNA yield and integrity, which were similar to controls

standard error of the mean. The differences among data were apparently due to the high degradation of the RNA from some samples. Regarding the RNA integrity, only the RNA from sections processed for TH immunohistochemistry (RIN = 5.7 ± 1.2), but not for immunofluorescence (RIN = 6.9 ± 0.2), showed a significantly ($p < 0.05$) lower RIN compared with the control group (Fig. 1b). However, the RIN value obtained after both rapid immunostaining protocols remained above 5; the minimum value required for RT-PCR studies (Schroeder et al. 2006).

By contrast, tissue sections processed for a 1-day (using a 1 h primary antibody incubation) immunofluorescence or immunohistochemistry methods showed a lower RNA yield (20.5 ± 6.7 ng/µl per section, $p > 0.05$ or 5.5 ± 1.7 ng/µl per section, $p < 0.05$, respectively) and lower RNA integrity (RIN = 5.2 ± 1.1 or RIN = 1 ± 0, respectively, $p < 0.05$) compared with control sections (Fig. 1a, b). However, only the RNA integrity obtained from the immunofluorescence-processed sections was acceptable for RT-PCR studies, whereas the RNA obtained from sections processed from the immunohistochemistry method was totally degraded. Similarly, an ordinary (using an o.n. primary antibody incubation) immunofluorescence or immunohistochemistry method decreased the RNA yield (15.7 ± 3.4 or 7.5 ± 1 ng/µl per section, respectively; $p < 0.05$) and integrity (RIN = 4.9 ± 1 or RIN = 1 ± 0, respectively; $p < 0.05$) compared with the control group (Fig. 1a, b). These RIN values indicated that the RNA integrity obtained after ordinary immunostaining methods are not acceptable for further RT-PCR studies. All together, our results showed that TH immunofluorescence staining preserves the RNA yield and integrity better than TH immunohistochemistry (immunoperoxidase) method in spite of whatever incubation times used. Additionally, when we compared different immunofluorescence protocols we confirmed that rapid, but not 1-day or ordinary, TH immunofluorescence staining allowed for obtaining similar RNA yield and integrity than the control group (Fig. 1c, d).

Effect of neutral red staining or rapid TH immunofluorescence on the RNA yield and integrity before LCM

Five tissue sections per animal containing the SN were processed for neutral red staining or rapid TH immunofluorescence (Fig. 2a, b). Then, the RNA obtained from scraped tissue sections was analyzed for the assessment of RNA yield and integrity (RIN). Compared with control (without staining) sections, tissue sections stained with neutral red showed similar RNA yield (42.1 ± 7.2 ng/µl per section, $p > 0.05$) but significantly lower RNA integrity (RIN = 6.3 ± 0.5; $p < 0.05$) (Fig. 2c, d). However, the RIN

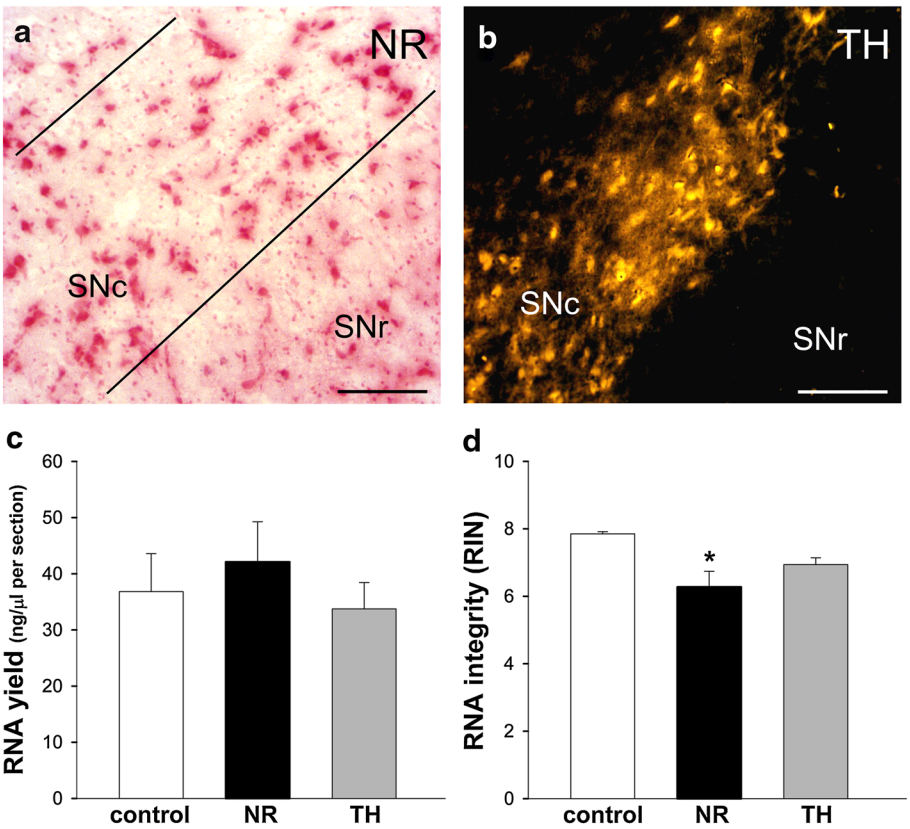

Fig. 2 Microphotographs showing rat substantia nigra (SN) sections processed with neutral red staining (**a**) or immunofluorescence (IF) against tyrosine hydroxylase (TH) (**b**). Neutral red staining and rapid TH-IF did not modify the RNA yield compared with control (unstained) sections (**c**). RNA from tissue sections processed for neutral red, but not for TH-IF, showed a decrease in integrity compared with RNA from control sections (**d**). However, the RIN value of the stained sections was higher than 5 showing a good quality of the RNA. The RNA yield was determined by dividing the concentration of RNA (ng/µl) per area (mm^2). The RNA integrity number (RIN) ranged from 1 to 10. Data represent mean ± standard error of the means (SEM). *$p \leq 0.05$ compared with the control group. One-way ANOVA and Bonferroni post hoc test. *SNc* substantia nigra pars compacta, *SNr* substantia nigra pars reticulata. *Scale bars* 150 µm

value obtained by neutral red stained sections remained above 5; the minimum value required for RT-PCR studies (Schroeder et al. 2006). In contrast, rapid TH immunofluorescence did not affect the RNA yield (33.7 ± 4.7 ng/µl per section, $p > 0.05$) and integrity (RIN = 6.9 ± 0.2, $p > 0.05$) compared with unstained tissue sections (Fig. 2c, d). Taken together, these data showed that both neutral red staining and rapid TH immunofluorescence can be used for LCM and gene expression studies. However, TH immunolabeling preserved better RNA integrity and it is a specific dopaminergic marker allowing for a more precise delimitation of the SN region compared with neutral red (Fig. 2a, b).

Effect of section thickness and slide type on tissue capture success and RNA yield, and integrity after LCM

Midbrain tissue sections with two different thicknesses (10 or 20 µm) and mounted onto two different slides (glass or PEN-membrane coated) were used to determine the best tissue preparation conditions for LCM. Tissue sections were stained with neutral red and the SN (1 mm^2) was microdissected. The capture success was assessed for each tissue section and LCM protocol as a percentage, and was calculated by dividing the dissected tissue area (after LCM process) by the selected tissue area (before LCM process). The collection microtube cap was checked after the LCM process to confirm the capture success (Table 1; Fig. 3a–f). Additionally, the RNA yield and the RIN were also calculated (Fig. 3g, h).

Ten micrometers-thick sections mounted on glass or PEN membrane-coated slides led to bad capture success (Table 1), since less than 50% of the selected tissue was dissected and catapulted. Observation of the collection microtube cap after LCM confirmed the bad capture success obtained (Fig. 3a). Regarding the RNA, 10 µm-thick sections showed a yield of 235.2 ± 37.1 pg/µl per mm^2 (glass slides) or 105.7 ± 15.2 pg/µl per mm^2 (PEN membrane-coated slides), and a RIN value of 1.7 ± 0.7 or 1.0, respectively, indicating that the RNA was totally degraded (Fig. 3g, h). These results showed that 10 µm-thick sections, regardless of the type of slide used, do not lead to the good tissue capture and RNA quality required for LCM and RT-PCR studies.

In contrast, a good capture success was obtained when 20 µm- thick sections mounted on glass slides were microdissected (Table 1). All the selected tissue was dissected and catapulted from the slides after the microdissection process (Fig. 3b–d). The RNA obtained from these tissue sections showed a yield of 456.2 ± 55.4 pg/µl per mm^2 and a RIN value of 6.3 ± 0.6 (Fig. 3g, h). Both results were significantly higher compared with those obtained from 10 µm-thick sections mounted on glass slides ($p < 0.05$).

Table 1 Capture success of the microdissected process using substantia nigra tissue sections with different thicknesses (10 or 20 µm) and mounted onto different slides (glass or PEN-membrane coated)

Section thickness (µm)	Slide type	Capture success
10	Glass	+
10	Membrane coated	+
20	Glass	+++
20	Membrane coated	++

The capture success was calculated as the percentage of selected tissue that was dissected by the laser: good (+++), 100%; fair (++),< 100%; and bad (+), <50%

These data suggested that 20 µm-thick sections mounted on glass slides could enable to obtain RNA with the quality necessary to combine LCM with RT-PCR analysis.

However, the slide type used appeared to be critical since 20 µm-thick sections mounted on PEN membrane-coated slides showed a fair tissue capture success after LCM (Table 1), since less than the 100% of the selected tissue was dissected and catapulted (Fig. 3e, f). In addition, the RNA yield obtained after laser microdissection of 20 µm-thick SN sections mounted on membrane slides (65 ± 10.4 pg/µl per mm^2) was significantly lower compared with the yield recovered using tissue sections (20 µm thick) mounted on glass slides ($p < 0.05$) (Fig. 3g). However, in spite of the low yield, the RNA obtained using membrane-coated slides showed a good quality (RIN = 6.3 ± 0.8), similar to that found when using glass slides (Fig. 3h), and it was compatible with gene expression studies. In summary, the results showed that 20 µm-thick sections mounted on glass slides allowed better tissue capture success and RNA yield compared with thinner sections (10 µm) or similar thick sections mounted on PEN membrane coated slides.

Effect of microdissected tissue quantity and RNA extraction method on RNA yield and integrity after LCM

Serial SN tissue sections were processed for rapid TH immunofluorescence and they were used to determine the optimal amount of microdissected tissue, and the most accurate RNA extraction method necessary for combined LCM and gene expression studies (Fig. 4a, b). A total area of 0.4 or 1 mm^2 of the SN was microdissected, and the RNA was extracted by the Trizol method (based on phase separation) or the Qiagen RNeasy Micro kit (based on separation by columns). Then, the RNA yield and RIN were calculated. After laser microdissection of 0.4 mm^2, the RNA obtained by the phase separation method showed a yield of 87.2 ± 31.1 pg/µl per mm^2 and a RIN value of 1.9 ± 0.9, indicating that RNA was totally degraded (Fig. 4c, d).

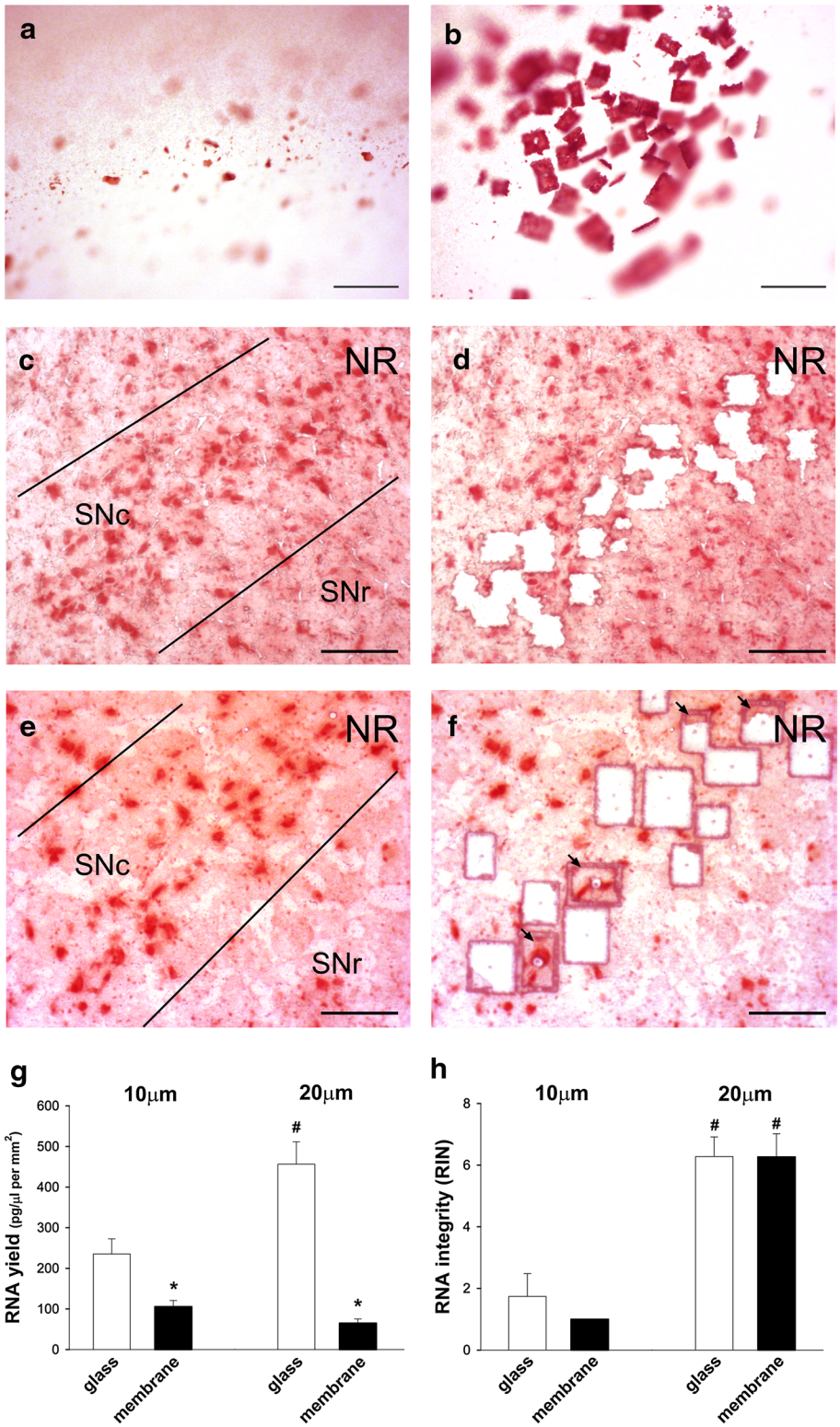

Fig. 3 Images of SN tissue dissected and catapulted to the microtube cap after LCM (**a**, **b**) and showing the differences between a bad (**a**) and good (**b**) capture success. Microphotographs of rat substantia nigra (SN; 20 µm thick) sections mounted on glass slides (c, **d**) or PEN membrane coated slides (**e**, **f**) and stained with neutral red. Comparison between images obtained before (**c**, **e**) and after (**d**, **f**) laser microdissection showed that glass slides allowed a better tissue capture success compared with membrane coated slides. The RNA obtained from 20 µm-thick tissue sections mounted on glass slides showed a greater yield compared with 10 µm-thick tissue sections mounted on glass slides (*hash*) and 20 µm-thick tissue sections mounted on PEN membrane-coated slides (*asterisk*) (**g**). The RNA obtained from 20 µm-thick tissue sections mounted on glass slides showed a higher RIN compared with RNA from 10 µm-thick tissue sections mounted on glass slides (*hash*), but similar to 20 µm-thick tissue sections mounted on PEN membrane-coated slides (**h**). The RNA yield was determined by dividing the concentration of RNA (pg/µl) per area (mm^2). The RNA integrity number (RIN) ranged from 1 to 10. Data represent mean ± standard error of the means (SEM). *$p \leq 0.05$ compared with glass slide. #$p \leq 0.05$ compared with 10 µm-thick. Two-way ANOVA and Bonferroni post hoc test. *SNc* substantia nigra pars compacta, *SNr* substantia nigra pars reticulata. *Scale bars* 150 µm

By contrast, the RNA extracted using the column-based method showed a similar yield (96.1 ± 7.4, $p > 0.05$), but a RINvalue was significantly higher (6.6 ± 0.5, $p < 0.05$) compared with the RNA obtained by the phase separation method (Fig. 4c, d). These results suggest the use of the column-based method to extract RNA with the quality required for RT-PCR studies of small microdissected areas. After laser microdissection of 1 mm^2 of tissue area, the RNA obtained using the phase separation method showed a yield of 287.3 ± 56.5 pg/µl per mm^2, which was

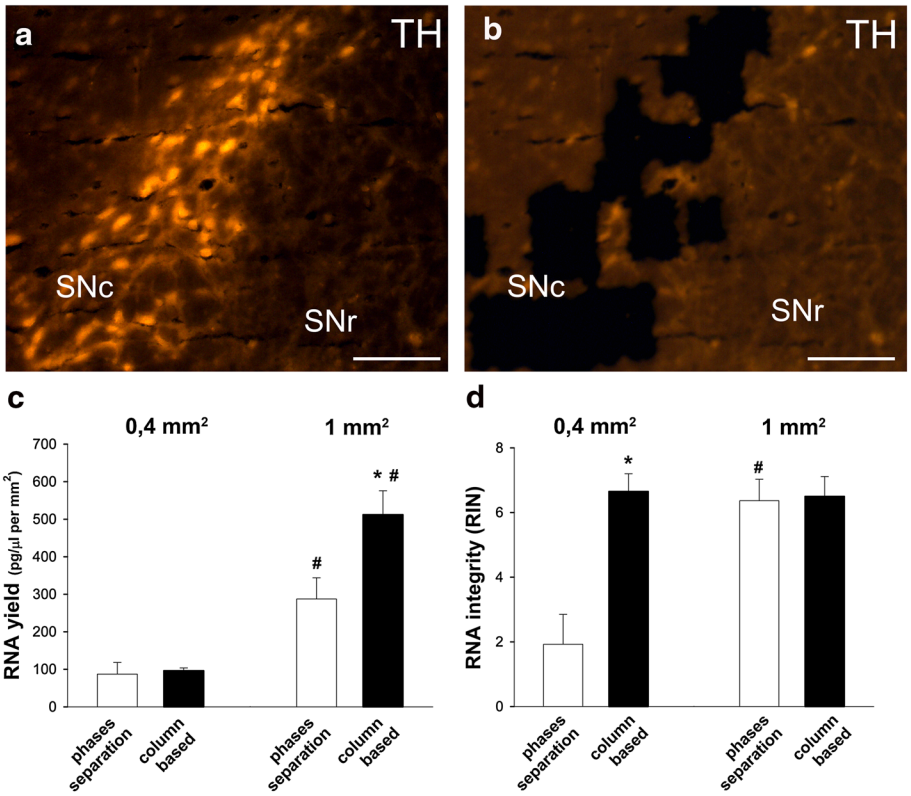

Fig. 4 Microphotographs showing rat substantia nigra (SN) sections processed for TH immunofluorescence before (**a**) and after (**b**) laser microdissection process. RNA obtained from 1 mm^2 tissue areas using a column-based method showed a higher yield compared with RNA from 0.4 mm^2 tissue areas processed by the same method (*hash*) or from 1 mm^2 tissue areas processed by a phase separation method (*asterisk*) (**c**). RNA obtained from 0.4 mm^2 tissue areas by a column-based method showed a higher RIN compared with RNA obtained from 0.4 mm^2 tissue areas and processed by a phase separation method (*asterisk*). Additionally, the RNA obtained from 1 mm^2 tissue areas by a phase separation method showed a higher RIN compared with RNA from 0.4 mm^2 tissue areas processed by a phase separation method (*hash*) (**d**). The RNA yield was determined by dividing the concentration of RNA (pg/µl) per area (mm^2). The RNA integrity number (RIN) ranged from 1 to 10. Data represent mean ± standard error of the means (SEM). *$p \leq 0.05$ compared with phase separation method. #$p \leq 0.05$ compared with 0.4 mm^2. Two-way ANOVA and Student–Newman–Keuls post hoc test. *SNc* substantia nigra pars compacta, *SNr* substantia nigra pars reticulata. *Scale bars* 150 µm

slightly, but not significantly ($p > 0.05$), higher compared with the yield obtained from 0.4 mm^2 microdissected areas (Fig. 4c). Additionally, the RNA integrity showed a RIN value of 6.4 ± 0.7, which was significantly higher compared with the RIN of RNA from 0.4 mm^2 microdissected areas (Fig. 4d), and was appropriated for subsequent gene expression studies (Schroeder et al. 2006).

The RNA obtained using the column-based method showed a significantly higher yield (512 ± 64 pg/µl per mm^2, $p < 0.05$) compared with the RNA yield obtained from the same microdissected area using the phase separation method (Fig. 4c). In addition, the RIN value (6.5 ± 0.6) was similar to the value showed by 1 mm^2 microdissected areas that were processed using the phase separation method (Fig. 4d). Finally, RNA obtained from tissue areas of 1 mm^2 using the column-based method showed a higher yield, but similar integrity, compared with 0.4 mm^2 of SN tissue area. Taken together, these data indicate that a column-based method is more suitable compared with the phase separation method to extract RNA from small and large microdissected tissue regions. However, a phase separation method may be used for obtaining RNA with the minimum quality required for gene expression studies when using large microdissected tissue regions.

Optimized laser capture microdissection protocol combined with RT-PCR for gene expression analysis in the substantia nigra

Two genes of the renin–angiotensin system and three genes specifically expressed by dopaminergic neurons were used to evaluate the success of combining LCM and RT-PCR for gene expression studies. The gene GAPDH was used as housekeeping. Firstly, we assessed the expression of these genes in ventral mesencephalic homogenates

(positive control) by RT-PCR analysis. We found that all these genes were expressed in the homogenates and they showed the following threshold cycle (Ct) values: 25.9 ± 0.7 (AT1 receptor), 24.5 ± 1.4 (AT2 receptor), 22 ± 0.05 (D2R), 19.5 ± 0.04 (DAT), 20.4 ± 0.1 (TH), and 15 ± 0.05 (GAPDH). The Ct value is inversely proportional to the level of gene expression, and it has been shown that genes with Ct values >7 Ct points larger than the Ct for the housekeeping gene are expressed at too low levels (Amisten 2016). Based on Amisten´s classification, AT1 and AT2 receptors were scarcely expressed in the ventral mesencephalic homogenates, whereas D2R, DAT and TH were, as expected, abundantly expressed.

Subsequently, all these genes were used to assess how our optimized LCM protocol works with transcripts showing low (i.e., AT1 and AT2 receptors) or high (i.e., TH, DAT and D2R) expression. As conclusion of the above-mentioned results, the optimized protocol for LCM consisted of tissue sections 20 µm-thick mounted on glass slides and processed for rapid TH immunofluorescence (Fig. 5a, b). A total tissue area of 1 mm^2 was microdissected using the PALM MicroBeam system and the RNA was extracted using a column-based method. The RT-PCR analysis confirmed that all of the genes studied were expressed in the healthy rat SN after LCM (Fig. 5c). The Ct values for each gene were: 35.9 ± 0.4 (AT1 receptor), 32.1 ± 0.3 (AT2 receptor), 27.2 ± 0.5 (D2R), 22 ± 0.3 (DAT), 23 ± 0.4 (TH), and 21.8 ± 0.4 (GAPDH). In addition, the expression of these genes was confirmed by loading the PCR products on agarose gels (Fig. 5c).

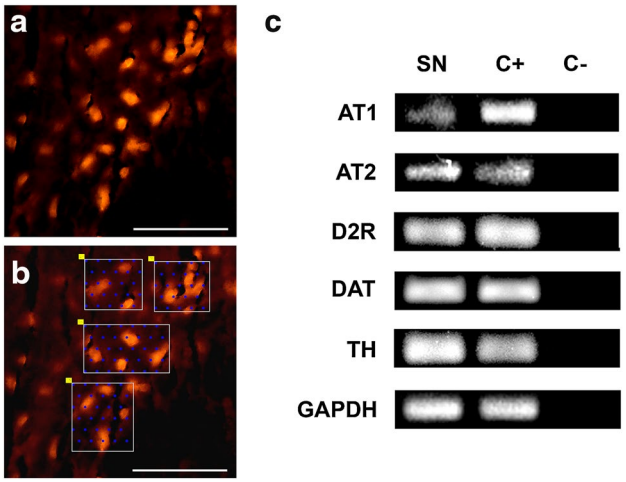

Fig. 5 Microphotographs from rat substantia nigra (SN) sections processed for TH immunofluorescence before the laser microdissection process (**a, b**). The area of interest is selected using the PALM RoboSoftware before microdissecction (**b**). Expression of AT1 and AT2 receptors, the dopaminergic markers D2R, TH, and DAT and the control gene GAPDH in the microdissected rat SN (1 mm^2) as determined by RT-PCR and agarose gel electrophoresis (**c**). Rat ventral mesencephalic homogenates were used as positive control (C+), and RT-PCR mixes (without tissue samples) were used as negative control (C−). *Scale bars* 150 µm

Discussion

In the present study, we developed a LCM protocol to obtain enough high-quality RNA for subsequent gene expression analysis. Although our study used SN tissue sections, the suggested LCM protocol could be applied to study other brain regions. RNA is a very labile biomolecule that is easily degraded during manipulation. Therefore, since LCM and gene expression studies work with low amounts of material, special cautions must be taken to preserve RNA yield and integrity, which are decisive for PCR analysis. The RNA yield and/or integrity, and thus gene expression studies, can be affected negatively by tissue manipulation, LCM process and RNA extraction. The present study has optimized these three critical steps, particularly for the PALM LCM system. Our results showed that the optimal LCM protocol required the use of 20 µm-thick tissue sections mounted on glass slides and processed for rapid TH immunofluorescence. Additionally, a total microdissected tissue area of 1 mm^2 and a column-based RNA extraction method led to the highest RNA yield and integrity. Using this optimized LCM protocol, we demonstrated the expression of two genes expressed at low levels in the healthy rat SN (i.e., AT1 and AT2 receptors). The present LCM protocol could be used to study the expression of numerous (either scarcely or abundantly expressed) genes in the different brain regions of mammals under both physiological and pathological conditions.

Effect of tissue staining on RNA yield and integrity before LCM

Tissue preparation before LCM, and particularly tissue staining, is a critical step for RNA preservation since it can be degraded by endogenous and environmental RNases. Therefore, during tissue manipulation all the reagents, materials and surfaces need to be decontaminated with RNase inhibitors (Esposito 2007; Field et al. 2011). In addition, some fixatives, that are required for tissue preservation, can interact with RNA affecting its stability. For these reasons, it is preferable to use frozen unfixed tissues (Curran et al. 2000; Decarlo et al. 2011; Kerman et al. 2006; Murray 2007), although paraffin-embedded tissue has also been used (Fedorowicz et al. 2009; Watanabe et al. 2015). When necessary, chemical fixatives like ethanol or acetone are used at low incubation times (Eltoum et al. 2002; Hernandez and Lloreta 2006). The use of conventional stains or

immunohistochemical techniques can identify specific cell populations. However, the protocols for these staining methods must be shortened to prevent RNA modification and/or degradation (Brown and Smith 2009; Decarlo et al. 2011; Murray 2007; Tangrea et al. 2011, Wang et al. 2006).

Our results showed that both neutral red staining and a rapid TH immunofluorescence method did not affect the RNA yield compared with unstained sections. In addition, only neutral red staining, but not TH immunolabeling, slightly decreased the RNA integrity compared with control sections. However, the RNA integrity obtained after both types of tissue staining was sufficiently good and compatible with subsequent RT-PCR studies (Schroeder et al. 2006). These results are consistent with previous studies that used general stains, such as neutral red, cresyl violet or hematoxyilin–eosin in kidney and brain tissue sections (Kerman et al. 2006; Yee et al. 2014). These authors showed a mildly decreased RNA integrity after tissue staining that allowed gene expression analysis.

However, when a precise delimitation of the tissue region or a subpopulation of cells is required, a general stain method must be replaced by immunohistochemical techniques. In the present study, we have demonstrated that combining immunohistochemistry and LCM requires shortened protocols to prevent RNA degradation. In addition, we have also observed that the immunofluorescence method preserve the RNA yield and integrity better than enzymatic immunohistochemical method. This result could be explained because immunofluorescence methods usually require less tissue manipulation compared with enzymatic immunohistochemical methods. Interestingly, we have developed a shortened immunofluorescence method for the dopaminergic marker TH. Our data showed that a rapid TH immunofluorescence preserves RNA integrity better than neutral red staining, and can also be used for combining LCM with gene expression studies. Moreover, since TH immunofluorescence delimites more precisely the borders of the SN, it will be more appropriate than neutral red for LCM studies in the SN.

Regarding the RNA yield, our results showed that it was not affected by either neutral red or rapid TH immunofluorescence. This is consistent with previous results obtained in hippocampus tissue sections (Vincent et al. 2002). However, Kerman et al. (2006) observed higher RNA yield using neutral red-or cresyl violet-stained tissue sections compared with using unstained sections. Since RNA concentration measurements do not take into account the integrity of RNA, the presence of fragmented RNA may lead to confusion. For that reason, both RNA yield and integrity have to be analyzed when a LCM protocol is being optimized.

Effect of tissue preparation conditions on tissue capture success and RNA yield and integrity after LCM

During the LCM process, the capture success depends on the tissue section thickness and the slide type (Curran et al. 2000; Decarlo et al. 2011; Espina et al. 2006). However, the effect of these parameters on RNA yield and integrity had not been studied previously. Our results showed that 10 µm-thick tissue sections, regardless of the slide type used (glass or PEN membrane-coated), are not adequate to capture microdissected tissue. The RNA yield was too low, and the RNA was totally degraded and not adequate for subsequent RT-PCR analysis. However, the capture success and RNA yield were higher using 20 µm-thick tissue sections than using 10 µm sections. This result could be explained by the lesser adhesion to the slide showed by 20 µm-thick tissue sections compared with 10 µm sections. Therefore, thicker tissue sections could facilitate tissue catapulting by the UV laser of the PALM system.

There is a previous study using the Arcturus LCM system that determined the effect of tissue thickness on the capture success (Espina et al. 2006), although RNA yield and integrity were not analyzed. In particular, Espina et al. (2006) described that 5 µm or thinner tissue sections did not allow for obtaining the tissue quantity required for further studies. Additionally, they showed that 15 µm or thicker tissue sections were not adequate for microdissection. The discrepancies with the present study could be explained by the LCM system and the laser type used. Whereas the Arcturus system possesses a low-energy infrared laser, the PALM system uses a high energy UV laser (Sluka et al. 2008), which can catapult thicker tissue sections compared with an infrared laser. In summary, this is the first study showing the effect of section thickness on RNA yield and integrity of microdissected tissue. Our results open the door to new studies using other tissues and microdissection systems. Our data suggest that the capture success is directly related to the yield and integrity of the obtained RNA.

Regarding the slide type, the PALM system can use glass or PEN membrane-coated slides (Lu and Szeto 2011). It has been claimed that membrane-coated slides make it possible to capture greater tissue areas with lower laser intensity and time compared with glass slides (Kummari et al. 2015; Sluka et al. 2008). However, our results showed that LCM of 20 µm-thick tissue sections mounted on glass slides led to higher capture success and RNA yield compared with those from sections mounted on PEN membrane-coated slides. However, RNA integrity was similar in glass and membrane slides and compatible with gene expression studies. The higher capture success and RNA yield obtained with glass slides compared with PEN-membrane slides could be due to the increase in adhesion between tissue and PEN-membrane slides.

Effect of microdissected tissue quantity and RNA extraction method on RNA yield and integrity after LCM

In LCM studies, two different type of extraction methods have been used to preserve the RNA yield and integrity: a phase separation method (i.e., Trizol) (Sluka et al. 2008) or a column-based method (i.e., RNeasy Micro kit) (Brown et al. 2013). We have found that for a small (0.4 mm^2) microdissected area, the RNA extraction method based on columns, but not the phase separation method, led to a good RNA quality compatible with subsequent RT-PCR studies. This RNA extraction method preserves the RNA integrity of low amounts of RNA obtained from small tissue areas. However, additional studies are necessary to process smaller tissue regions or individual isolated cells. Regarding larger microdissected areas (1 mm^2), the integrity of the RNA extracted by a column-based or a phaseseparation method was similar and enough for further gene expression studies. However, the column-based RNA extraction method led to higher yield compared with the phase separation method. The present results indicate that column-based RNA extraction methods are more appropriate than phase separation methods for RNA extraction from either small or large microdissected areas. However, phase separation methods are widely used for preparation of total homogenates of tissues, and may be used for LCM studies of large microdissected tissue areas.

Optimized laser capture microdissection protocol combined with RT-PCR for gene expression analysis in the substantia nigra

In the present study, we showed that AT1 and AT2 receptors are expressed at low levels in ventral mesencephalic homogenates from young control rats. This result is in agreement with the previous results obtained at our laboratory using molecular biology techniques (Villar–Cheda et al. 2010, 2012). These results were confirmed using immunohistochemical studies that showed the localization of AT1 and AT2 receptors within the SN of rats, monkeys, and humans (Garrido-Gil et al. 2013; Joglar et al. 2009; Rodriguez–Pallares et al. 2008). These receptors are expressed at low levels in healthy young brains and increase in pathological conditions such as those contributing to the development of Parkinson's disease (for review see Labandeira-Garcia et al. 2011, 2012, 2014). Their low expression in control animals is a handicap for studies using a low amount of tissue such as LCM methods. For this reason, the optimization of the LCM protocol is critical. Interestingly, the present validated LCM protocol combined with RT-PCR confirmed that AT1 and AT2 receptors are expressed in the healthy rat SN. In addition, we have demonstrated that our LCM and RT-PCR combined protocol is also appropriate for transcripts that are highly expressed, such as the dopaminergic markers TH, DAT, and D2R. The present methodology is particularly interesting. Firstly, because LCM plus RT-PCR studies prevent the problems associated with the use of possible unspecific antibodies during immunohistochemical analysis. Secondly, because LCM plus RT-PCR analysis allows for the study of an isolated tissue region of interest, while tissue homogenates commonly used for biochemical studies usually include unwanted adjacent structures.

Acknowledgements The authors thank Pilar Aldrey, Cristina Gianzo, Iria Novoa and Jose Trillo for their technical assistance. The present study was supported by Spanish Ministry of Economy and Competitiveness (BFU2015-70523), Spanish Ministry of Health (RD12/0019/0020, RD16/0011/0016 and CIBERNED), Galician Government (XUGA) and FEDER (Regional European Development Fund).

Compliance with ethical standards

Conflict of interest The authors declare that they have no conflict of interest.

References

Amisten S (2016) Quantification of the mRNA expression of G protein-coupled receptors in human adipose tissue. In: Shukla AK (ed) Methods in cell biology, G protein-coupled receptors: signaling, trafficking and regulation, vol 132, 1st edn. Academic Press, Elservier, Cambridge, pp 73–108

Brown AL, Smith DW (2009) Improved RNA preservation for immunolabeling and laser microdissection. RNA 15:2364–2374. doi:10.1261/rna.1733509

Brown AL, Day TA, Dayas CV, Smith DW (2013) Purity and enrichment of laser-microdissected midbrain dopamine neurons. Biomed Res Int 2013:747938. doi:10.1155/2013/747938

Cheng L, Zhang S, MacLennan GT, Williamson SR, Davidson DD, Wang M, Jones TD, Lopez-Beltran A, Montironi R (2013) Laser-assisted microdissection in translational research: theory, technical considerations, and future applications. Appl Immunohistochem Mol Morphol 21:31–47. doi:10.1097/PAI.0b013e31824d0519

Curran S, McKay JA, McLeod HL, Murray GI (2000) Laser capture microscopy. Mol Pathol 53:64–68

Damier P, Hirsch EC, Agid Y, Graybiel AM (1999) The substantia nigra of the human brain. II. Patterns of loss of dopamine-containing neurons in Parkinson's disease. Brain 122(Pt 8):1437–1448

Decarlo K, Emley A, Dadzie OE, Mahalingam M (2011) Laser capture microdissection: methods and applications. Methods Mol Biol 755:1–15. doi:10.1007/978-1-61779-163-5_1

Elkahloun AG, Hafko R, Saavedra JM (2016) An integrative genome-wide transcriptome reveals that candesartan is neuroprotective and a candidate therapeutic for Alzheimer's disease. Alzheimers Res Ther 28(8):5. doi:10.1186/s13195-015-0167-5

Eltoum IA, Siegal GP, Frost AR (2002) Microdissection of histologic sections: past, present, and future. Adv Anat Pathol 9:316–322

Emmert-Buck MR, Bonner RF, Smith PD, Chuaqui RF, Zhuang Z, Goldstein SR, Weiss RA, Liotta LA (1996) Laser capture microdissection. Science 274:998–1001

Espina V, Wulfkuhle JD, Calvert VS, VanMeter A, Zhou W, Coukos G, Geho DH, Petricoin EF 3rd, Liotta LA (2006) Laser-capture microdissection. Nat Protoc 1:586–603

Esposito G (2007) Complementary techniques: laser capture microdissection–increasing specificity of gene expression profiling of cancer specimens. Adv Exp Med Biol 593:54–65

Fedorowicz G, Guerrero S, Wu TD, Modrusan Z (2009) Microarray analysis of RNA extracted from formalin-fixed, paraffin-embedded and matched fresh-frozen ovarian adenocarcinomas. BMC Med Genom 2:23. doi:10.1186/1755-8794-2-23

Fend F, Raffeld M (2000) Laser capture microdissection in pathology. J Clin Pathol 53:666–672

Field LA, Deyarmin B, Shriver CD, Ellsworth DL, Ellsworth RE (2011) Laser microdissection for gene expression profiling. Methods Mol Biol 755:17–45. doi:10.1007/978-1-61779-163-5_2

Garrido-Gil P, Valenzuela R, Villar-Cheda B, Lanciego JL, Labandeira-Garcia JL (2013) Expression of angiotensinogen and receptors for angiotensin and prorenin in the monkey and human substantia nigra: an intracellular renin-angiotensin system in the nigra. Brain Struct Funct 218:373–388. doi:10.1007/s00429-012-0402-9

Gonzalez-Hernandez T, Barroso-Chinea P, De La Cruz Muros I, Del Mar Perez-Delgado M, Rodriguez M (2004) Expression of dopamine and vesicular monoamine transporters and differential vulnerability of mesostriatal dopaminergic neurons. J Comp Neurol 479:198–215

Gonzalez-Hernandez T, Cruz-Muros I, Afonso-Oramas D, Salas-Hernandez J, Castro-Hernandez J (2010) Vulnerability of mesostriatal dopaminergic neurons in Parkinson's disease. Front Neuroanat 4:140. doi:10.3389/fnana.2010.00140

Haber SN (2014) The place of dopamine in the cortico-basal ganglia circuit. Neuroscience 282C:248–257. doi:10.1016/j.neuroscience.2014.10.008

Hernandez S, Lloreta J (2006) Manual versus laser micro-dissection in molecular biology. Ultrastruct Pathol 30:221–228

Joglar B, Rodriguez-Pallares J, Rodriguez-Perez AI, Rey P, Guerra MJ, Labandeira-Garcia JL (2009) The inflammatory response in the MPTP model of Parkinson's disease is mediated by brain angiotensin: relevance to progression of the disease. J Neurochem 109:656–669. doi:10.1111/j.1471-4159.2009.05999.x

Kerman IA, Buck BJ, Evans SJ, Akil H, Watson SJ (2006) Combining laser capture microdissection with quantitative real-time PCR: effects of tissue manipulation on RNA quality and gene expression. J Neurosci Methods 153:71–85

Kim T, Lim CS, Kaang BK (2015) Cell type-specific gene expression profiling in brain tissue: comparison between TRAP, LCM and RNA-seq. BMB Rep 48:388–394

Korabecna M, Steiner P, Jirkovska M (2016) DNA from microdissected tissues may be extracted and stored on microscopic slides. Neoplasma 63:518–522. doi:10.4149/neo_2016_404

Kummari E, Guo-Ross SX, Eells JB (2015) Laser capture microdissection—a demonstration of the isolation of individual dopamine neurons and the entire ventral tegmental area. J Vis Exp. doi:10.3791/52336

Labandeira-Garcia JL, Rodriguez-Pallares J, Villar-Cheda B, Rodriguez-Perez AI, Garrido-Gil P, Guerra MJ (2011) Aging, angiotensin system and dopaminergic degeneration in the substantia nigra. Aging Dis 2:257–274

Labandeira-Garcia JL, Rodriguez-Pallares J, Rodriguez-Perez AI, Garrido-Gil P, Villar-Cheda B, Valenzuela R, Guerra MJ (2012) Brain angiotensin and dopaminergic degeneration: relevance to Parkinson's disease. Am J Neurodegener Dis 1:226–244

Labandeira-Garcia JL, Garrido-Gil P, Rodriguez-Pallares J, Valenzuela R, Borrajo A, Rodriguez-Perez AI (2014) Brain renin-angiotensin system and dopaminergic cell vulnerability. Front Neuroanat 8:67. doi:10.3389/fnana.2014.00067

Li J, Xing X, Li D, Zhang B, Mutch DG, Hagemann IS, Wang T (2017) Whole-genome DNA methylation profiling identifies epigenetic signatures of uterine carcinosarcoma. Neoplasia 19:100–111. doi:10.1016/j.neo.2016.12.009

Lu JX, Szeto CC (2011) Gene expression using the PALM system. Methods Mol Biol 755:47–56. doi:10.1007/978-1-61779-163-5_3

Murray GI (2007) An overview of laser microdissection technologies. Acta Histochem 109:171–176

Rodriguez-Pallares J, Rey P, Parga JA, Munoz A, Guerra MJ, Labandeira-Garcia JL (2008) Brain angiotensin enhances dopaminergic cell death via microglial activation and NADPH-derived ROS. Neurobiol Dis 31:58–73. doi:10.1016/j.nbd.2008.03.003

Schroeder A, Mueller O, Stocker S, Salowsky R, Leiber M, Gassmann M, Lightfoot S, Menzel W, Granzow M, Ragg T (2006) The RIN: an RNA integrity number for assigning integrity values to RNA measurements. BMC Mol Biol 7:3. doi:10.1186/1471-2199-7-3

Sluka P, O'Donnell L, McLachlan RI, Stanton PG (2008) Application of laser-capture microdissection to analysis of gene expression in the testis. Prog Histochem Cytochem 42:173–201. doi:10.1016/j.proghi.2007.10.001

Tangrea MA, Mukherjee S, Gao B, Markey SP, Du Q, Armani M, Kreitman MS, Rosenberg AM, Wallis BS, Eberle FC, Duncan FC, Hanson JC, Chuaqui RF, Rodriguez-Canales J, Emmert-Buck MR (2011) Effect of immunohistochemistry on molecular analysis of tissue samples: implications for microdissection technologies. J Histochem Cytochem 59:591–600. doi:10.1369/0022155411404704

Villar-Cheda B, Rodriguez-Pallares J, Valenzuela R, Munoz A, Guerra MJ, Baltatu OC, Labandeira-Garcia JL (2010) Nigral and striatal regulation of angiotensin receptor expression by dopamine and angiotensin in rodents: implications for progression of Parkinson's disease. Eur J Neurosci 32:1695–1706. doi:10.1111/j.1460-9568.2010.07448.x

Villar-Cheda B, Valenzuela R, Rodriguez-Perez AI, Guerra MJ, Labandeira-Garcia JL (2012) Aging-related changes in the nigral angiotensin system enhances proinflammatory and pro-oxidative markers and 6-OHDA-induced dopaminergic degeneration. Neurobiol Aging 33(204):e201–e211. doi:10.1016/j.neurobiolaging.2010.08.006

Vincent VA, DeVoss JJ, Ryan HS, Murphy GM Jr (2002) Analysis of neuronal gene expression with laser capture microdissection. J Neurosci Res 69:578–586

Wang H, Owens JD, Shih JH, Li MC, Bonner RF, Mushinski JF (2006) Histological staining methods preparatory to laser capture microdissection significantly affect the integrity of the cellular RNA. BMC Genom 7:97

Watanabe T, Kato A, Terashima H, Matsubara K, Chen YJ, Adachi K, Mizuno H, Suzuki M (2015) The PFA-AMeX method achieves a good balance between the morphology of tissues and the quality of RNA content in DNA microarray analysis with laser-capture microdissection samples. J Toxicol Pathol 28:43–49. doi:10.1293/tox.2014-0045

Yee JY, Limenta LM, Rogers K, Rogers SM, Tay VS, Lee EJ (2014) Ensuring good quality RNA for quantitative real-time PCR isolated from renal proximal tubular cells using laser capture microdissection. BMC Res Notes 7:62. doi:10.1186/1756-0500-7-62